PHYSOR 2002, Seoul, Korea, October 7-10, 2002

TRANSPORT EFFECTS FOR SOURCE-OSCILLATED PROBLEMS IN SUBCRITICAL SYSTEMS

S. Dulla, P. Ravetto, M.M. Rostagno
Politecnico di Torino, Dipartimento di Energetica,
Corso Duca degli Abruzzi, 24 - 10129 Torino, Italy
dulla@polito.it, ravetto@polito.it, rostagno@athena.polito.it

ABSTRACT

The transport equation is solved in the frequency domain for two-dimensional source-driven systems, using the discrete-ordinate method. The objective of the work is the determination of the importance of transport effects in subcritical systems driven by an oscillated neutron source. Some problems connected to the application of synthetic acceleration procedures for the solution of the transport equation in the frequency domain are addressed. Results presented allow to study transport effects for systems having different geometrical and material characteristics and for different values of the frequency of the source.

1. INTRODUCTION

A great deal of theoretical and experimental work is being carried out at present to establish the feasibility of the accelerator-driven concept. Experiments are under way in subcritical facilities to investigate the interaction between source and blanket and to study the neutronic performance of the system. Some experiments are run or proposed in source pulsed or oscillated mode. Therefore, it is of interest to investigate physical features of the neutron kinetics of subcritical systems in presence of source oscillations. This work is a contribution to the MUSE project [1] supported by the European Union in the Fifth Framework Program; the experimental activity is currently under way at CEN-Cadarache, CEA, France. The experiments should evidence the most important physical aspects that need to be taken into consideration for subcritical reactors. Furthermore, oscillated methods have also been proposed to monitor the reactivity of source-driven subcritical systems [2].

Since source neutrons generated through the spallation process are characterized by high energies, transport effects may become important in the physics of accelerator-driven systems. The present work is devoted to investigate the role of transport effects in different physical conditions in the frequency domain. The solution of the transport equation in the frequency domain yields information on the response of the system injected by a source characterized by a given frequency in the time domain. The transport equation is solved by the discrete ordinate scheme to determine the persistent contribution to the solution in a system injected by an oscillated source in two-dimensional $x - y$ geometry. Transport results

are then compared with diffusion for different materials and geometrical configurations to evidence the situations for which the diffusion model might be inadequate.

2. TRANSPORT MODEL IN THE FREQUENCY DOMAIN

2.1 The basic equations

It is supposed that an isotropic oscillated source is injecting neutrons within a two-dimensional subcritical system according to the law:

$$S(x,y,t) = S_0(x,y)e^{i\omega t}. \tag{1}$$

Since the system is supposed to be subcritical, the flux $\varphi(x,y,\hat{\Omega},t)$ which is solution of the neutron transport equation is expected to show an asymptotic behavior of the form $\varphi(x,y,\hat{\Omega},t) = \phi(x,y,\hat{\Omega})e^{i\omega t}$, where $\phi(x,y,\hat{\Omega})$ is the persistent shape of the neutron flux in response to the oscillated part of a neutron source, once the initial transient is estinguished. In multigroup problems ϕ is to be interpreted as a vector, whose components are the persistent fluxes in each energy group. However, for simplicity, only the one-group formulation is presented in the following. By direct substitution into the time-dependent transport equation for φ and by elimination of the common exponential factor, the space distribution $\phi(x,y,\hat{\Omega})$ of the response satisfies the following equation:

$$\hat{\Omega}\cdot\boldsymbol{\nabla}\phi(x,y,\hat{\Omega}) + \left[\Sigma(x,y) + \frac{i\omega}{v}\right]\phi(x,y,\hat{\Omega}) = \Theta_s\left[\phi\right] + \Theta_f\left[\phi\right] + \frac{1}{4\pi}S_0(x,y), \tag{2}$$

where $\Theta_s\left[\phi\right]$ and $\Theta_f\left[\phi\right]$ are the scattering and fission sources, respectively, according to the following definitions

$$\begin{aligned}\Theta_s\left[\phi\right] = \oint d\hat{\Omega}'\phi(x,y,\hat{\Omega}')\Sigma_s(x,y,\hat{\Omega}'\cdot\hat{\Omega}) = \sum_{n=0}^{L}\sum_{\beta=-n}^{n}\sigma_n(x,y)\phi_n^{\beta}(x,y)Y_n^{\beta}(\hat{\Omega}),\\ \Theta_f\left[\phi\right] = \frac{1}{4\pi}\oint d\hat{\Omega}'\phi(x,y,\hat{\Omega}')\nu\Sigma_f(x,y).\end{aligned} \tag{3}$$

The above definitions account for anisotropic scattering emissions and an expansion in terms of spherical harmonics is used, σ_n being the angular moments of the scattering cross section and ϕ_n^{β} the spherical harmonics moments of ϕ, as

$$\phi_n^{\beta}(x,y) = \oint d\hat{\Omega}\phi(x,y,\hat{\Omega})Y_n^{\beta *}(\hat{\Omega}). \tag{4}$$

Anisotropy effects in the collision term may become important in spallation-source driven systems, owing to the presence of very high energy neutrons.

The function $\phi(x,y,\hat{\Omega})$ takes complex values, owing to the fact that the apparent total cross section of the system in the frequency domain is complex. Its amplitude and phase

give all the physical information on the persistent response to a source having a given frequency ω. The behavior of ϕ in dependence of the frequency ω yields full information on the spatial propagation phenomena following any oscillated source signal.

2.2 The numerical solution

Equation (2) above is solved by a source iteration procedure [3];

$$\begin{aligned}&\hat{\Omega}\cdot\boldsymbol{\nabla}\phi^{(n)}(x,y,\hat{\Omega})+\left[\Sigma(x,y)+\frac{i\omega}{v}\right]\phi^{(n)}(x,y,\hat{\Omega})\\&=\Theta_s\left[\phi^{(n-1)}\right]+\Theta_f\left[\phi^{(n-1)}\right]+\tfrac{1}{4\pi}S_0(x,y)\equiv Q^{(n)}(x,y),\qquad\qquad\phi^{(0)}(x,y)=0,\end{aligned}\tag{5}$$

where n indicates the iteration order. The angular variable in Eq. (5) is discretized here according to the standard discrete ordinate scheme with diamond differencing. For physical configurations of interest in the applications, the iterative procedure may be very slowly converging. Hence, an acceleration procedure usually becomes necessary. In the present work a synthetic technique based on lower-order discrete ordinate models is used [4]. Such a technique is particularly suited to treat problems with anisotropic scattering, since it allows to accelerate higher order moments of the solution, while standard diffusion synthetic methods accelerate only the zero-th and first order moments. It must be noted that ϕ is a complex number, and this aspect requires a particular care for the application of algorithm.

2.3 The study of the synthetic acceleration procedure

In order to study the performance of an iteration technique, it is useful to refer to an infinite homogeneous medium characterized by a constant total cross section σ and by isotropic scattering, thus allowing the use of the Fourier transform from the geometrical 2D $\mathbf{r}$-space into the transformed 2D $\boldsymbol{\lambda}$-space ($\boldsymbol{\lambda}=(\lambda_x,\lambda_y)$). Results for this idealized configuration give indications on what is to be expected in more realistic situations.

The steady-state problem is considered at first. Each source iteration requires the solution of the discrete ordinate system of equations in the form

$$\hat{\Omega}_m\cdot\nabla\phi(\mathbf{r},\hat{\Omega}_m)+\sigma\phi(\mathbf{r},\hat{\Omega}_m)=\frac{1}{4\pi}\left[\sigma_s\Phi(\mathbf{r})+S_0(\mathbf{r})\right]\equiv\frac{1}{4\pi}Q(\mathbf{r}),\qquad m=1,2,...,N,\tag{6}$$

where the iteration index is dropped, m numbers the discrete directions and $\mathbf{r}=(x,y)$. The following quadrature formula needs to be introduced:

$$\oint d\hat{\Omega}f(\mathbf{r},\hat{\Omega})\cong\frac{1}{4}\sum_m w_m f_m(\mathbf{r},\hat{\Omega}_m).\tag{7}$$

Applying the Fourier transform to Eqs. (6), one obtains:

$$(i\lambda_x\mu_m + i\lambda_y\eta_m)\,\tilde{\phi}(\boldsymbol{\lambda},\hat{\Omega}_m) + \sigma\tilde{\phi}(\boldsymbol{\lambda},\hat{\Omega}_m) = \frac{1}{4\pi}\tilde{Q}(\boldsymbol{\lambda}), \qquad m = 1,2,...,N. \quad (8)$$

The transformed angular flux can be isolated and using Eq. (7) the scalar flux can be constructed as:

$$\tilde{\Phi}(\boldsymbol{\lambda}) = \frac{1}{4}\sum_m \frac{w_m}{i\lambda_x\mu_m + i\lambda_y\eta_m + \sigma}\frac{1}{4\pi}\tilde{Q}(\boldsymbol{\lambda}). \quad (9)$$

Consequently, the operator on which the iteration procedure is based is the following:

$$\mathcal{A}_N(\boldsymbol{\lambda}) = \frac{1}{4}\sigma_s\sum_m \frac{w_m}{i\lambda_x\mu_m + i\lambda_y\eta_m + \sigma}. \quad (10)$$

Its spectral radius is just the number of secondaries per collision σ_s/σ. It is clear that the procedure can be very slow-converging for cases characterized by values of σ_s/σ close to unity.

Synthetic acceleration is a well assessed technique in neutron transport [3]. The iteration is accelerated by using the results of a low order transport problem, whose source is the difference between the last two iterations. Of course, the benefit of the acceleration must be established in terms of computational effort rather than in terms of the reduction of the number of iteration required to reach convergence, since one accelerated iteration is obviously computationally more expensive than just a free source iteration.

If for instance an S_8 problem is considered, different acceleration schemes can be defined. The simplest one uses as lower order model simply the S_2 algorithm, thus extending the classical diffusion synthetic method. In this case the operator on which the S_2-accelerated iteration process, denoted by $S_{8[2]}$, is based turns out as:

$$\mathcal{A}_{8[2]}(\boldsymbol{\lambda}) = \frac{\sigma_s(A_8(\boldsymbol{\lambda}) - A_2(\boldsymbol{\lambda}))}{(1 - \sigma_s A_2(\boldsymbol{\lambda}))}. \quad (11)$$

A more sophisticated method accelerates the S_8 solution using S_4, which, on its turn, is accelerated by the S_2 equation [5]. Such a procedure is thus denoted by $S_{8[4-2]}$. This amounts to using the following operator:

$$\mathcal{A}_{8[4-2]}(\boldsymbol{\lambda}) = \frac{\sigma_s(A_8(\boldsymbol{\lambda}) - A_4(\boldsymbol{\lambda})) + \sigma_s^2(A_8(\boldsymbol{\lambda})A_4(\boldsymbol{\lambda}) - A_8(\boldsymbol{\lambda})A_2(\boldsymbol{\lambda}))}{(1 - \sigma_s A_2(\boldsymbol{\lambda}))}. \quad (12)$$

The amplitudes of these transformed operators take their maxima along $\lambda_x = \lambda_y$ [6].

The solution in the frequency domain poses new problems. The operator in the Fourier transformed space on which the iteration process is based can be deduced from Eq. (10) by

introduction of the frequency-dependent cross section:

$$\mathcal{A}_N(\boldsymbol{\lambda}) = \frac{1}{4}\sigma_s \sum_m \frac{w_m}{i\lambda_x\mu_m + i\lambda_y\eta_m + i\dfrac{\omega}{v} + \sigma}. \tag{13}$$

For values of ω of the order of σv, the operator changes its behavior in the $\boldsymbol{\lambda}$-space with respect to the steady state case. The spectral radius is determined by the maximum value of its amplitude, which is reached along the $\boldsymbol{\lambda}$ axes. Figure 1 reports graphs of the free and accelerated amplitude of the operators, which show that the spectral radius of the free operator is reduced by the presence of the frequency term. It is also clear that in high-frequency conditions for the material case considered the acceleration has no positive effect in speeding up the process. Figure 2 reports a typical comparison of the errors in free and accelerated calculations against the number of iterations and the computational effort. Table 1 shows the effectiveness of the acceleration procedure in dependence of the frequency for a simple geometrical configuration, a homogeneous square having and edge of 20 m.f.p., reporting the ratio ρ_{it} between the number of iterations needed to obtain convergence in each calculation and the maximum number of iterations in all calculations, and similarly the ratio ρ_t for computing times.

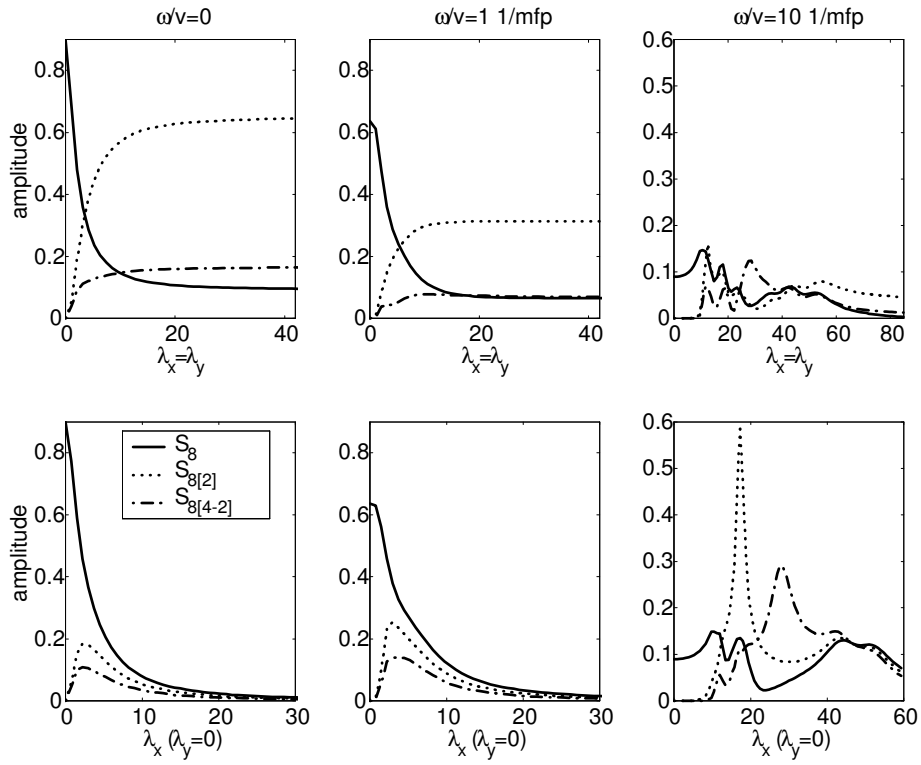

Fig. 1: Amplitude of free and accelerated operators corresponding to different frequencies ($c = 0.9$).

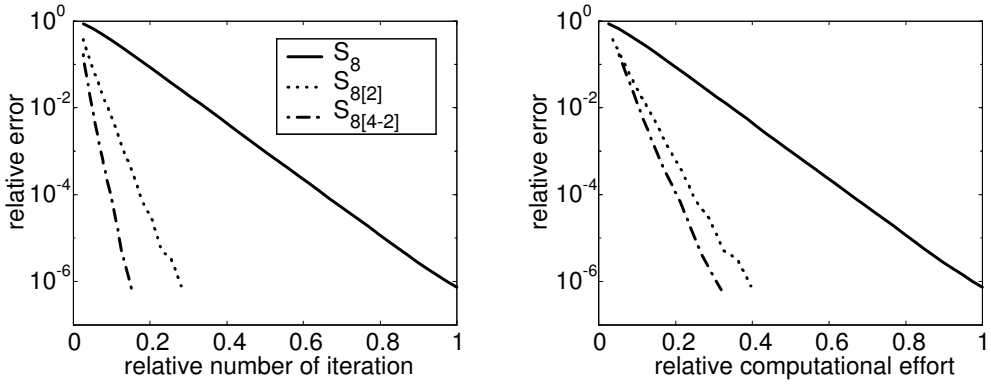

Fig. 2: Effectiveness of different acceleration methods compared to free source iteration ($\sigma = 1$, $c = 0.9$, $\omega = 0$).

Table 1: Effectiveness of the acceleration procedure for different values of ω/v ($\sigma = 1$, $c = 0.9$).

	S_8		$S_{8[4-2]}$	
$\omega/v\ [mfp^{-1}]$	ρ_{it}	ρ_t	ρ_{it}	ρ_t
0	1.00	1.00	0.08	0.28
10^{-3}	1.00	1.00	0.08	0.28
10^{-1}	1.00	1.00	0.08	0.28
1	0.35	0.35	0.08	0.28
10	0.08	0.09	0.08	0.28

3. RESULTS

Calculations are carried out in order to evidence transport effects in different physical configurations taking into consideration the amplitude and the phase of the response. Some selected results are discussed in the following. The first set of results studies the convergence trend of the discrete ordinate scheme for different source and material properties, with special regard to the appearance of ray effects in low-order models. Ray effect phenomena are shown for amplitude and phase in Figs. 3 and 4. Different angular orders are compared in Fig. 3, while S_8 results for different values of the number of secondaries per collision are presented in Fig. 4. For all cases the source is a 0.4 m.f.p. edge square

symmetrically located within the domain.

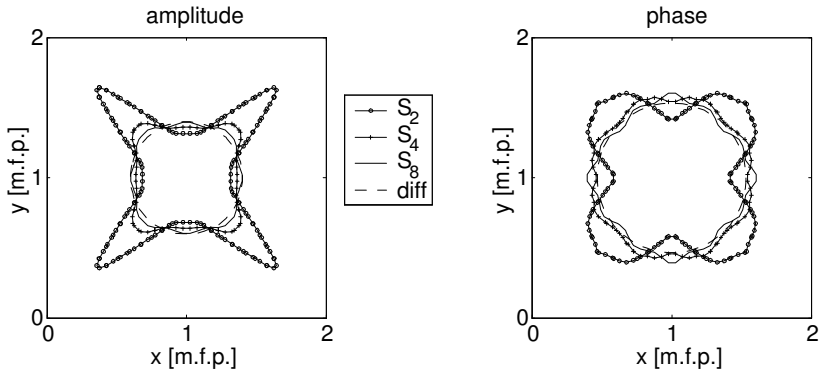

Fig. 3: Appearance of ray effect for different angular approximations ($c = 0.5$, $\omega/v = 0.1\ mfp^{-1}$).

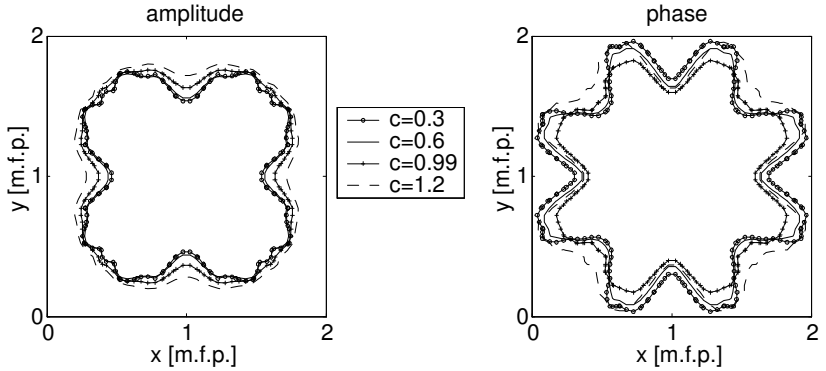

Fig. 4: Appearance of ray effect for different values of the number of secondaries per collision (S_8 approximation, $\omega/v = 0.1\ mfp^{-1}$).

The following Figs. 5 through 9 report the study on the extent of transport effects as compared to the diffusion model. The diffusion coefficient is assumed coherently with P_1 formalism, as $D = 1/(3\Sigma)$. The material considered is homogeneous and characterized by a source symmetrically located and uniformly distributed in a square having an edge equal to 1/2 the edge of the system itself. Figures 5 and 6 evidence the effect of the geometrical dimensions in determining the role of transport effects; Figs. 6 and 7 show the effect of the number of secondaries per collision, while Figs. 7, 8 and 9 compare results for different frequencies of the source. As one might expect, large discrepancies can appear when considering either optically thin systems or highly absorbing materials or when high frequency phenomena need to be accounted for, thus evidencing the inadequacy of the

diffusion model in foreseeing both the amplitude and the phase of the response. In high frequency cases, spatially oscillatory phenomena appear in the transport solution which are not present in the diffusion model.

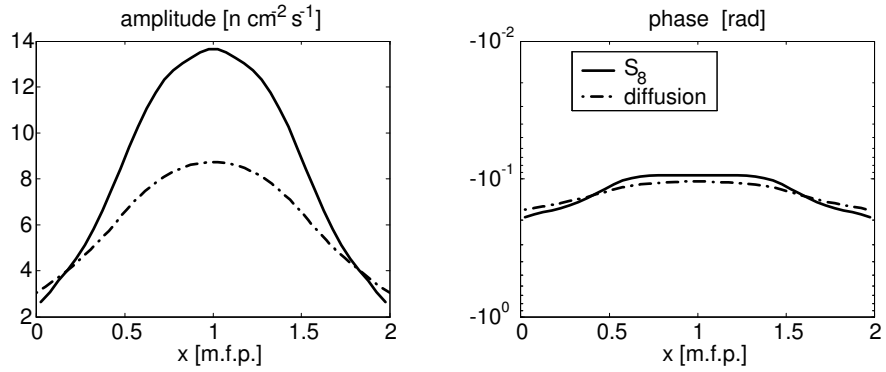

Fig. 5: Transport and diffusion solutions for an optically thin system ($c = 0.9$, $\omega/v = 0.1$ mfp^{-1}).

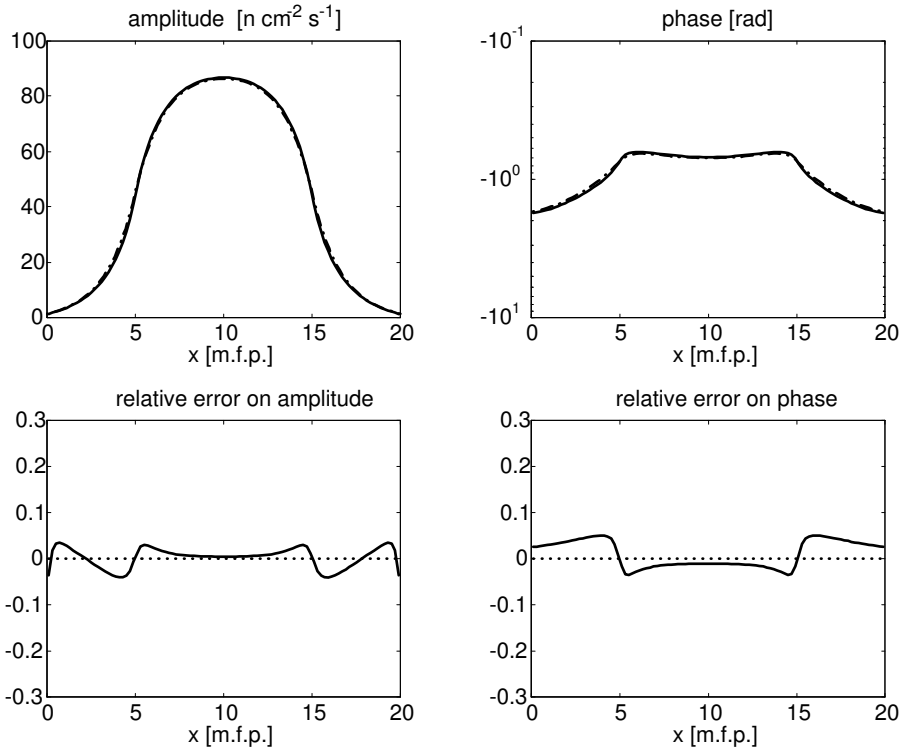

Fig. 6: Transport and diffusion solutions for an optically large system and relative differences ($c = 0.9$, $\omega/v = 0.1$ mfp^{-1}).

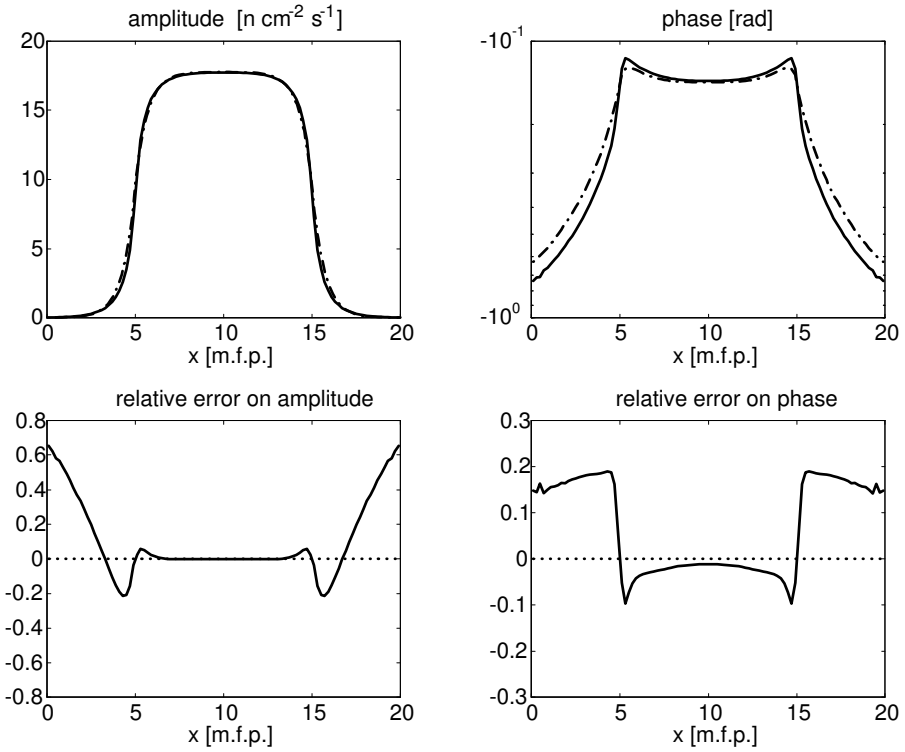

Fig. 7: Transport and diffusion solutions for an optically thick system and relative differences ($c = 0.3, \omega/v = 0.1\ mfp^{-1}$).

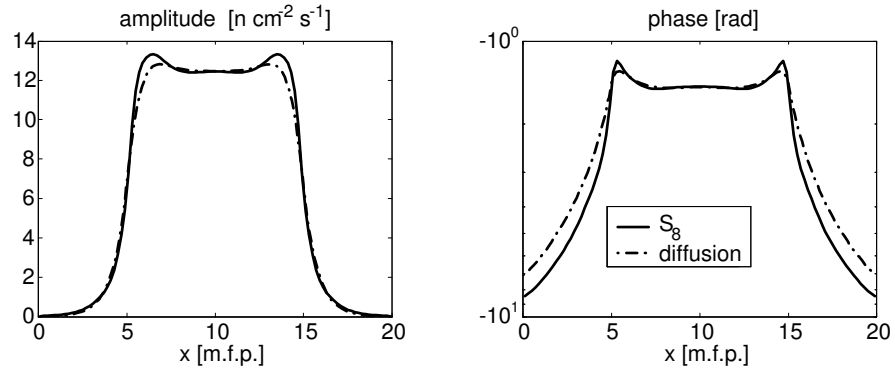

Fig. 8: Comparison between transport and diffusion solutions ($c = 0.9, \omega/v = 1\ mfp^{-1}$).

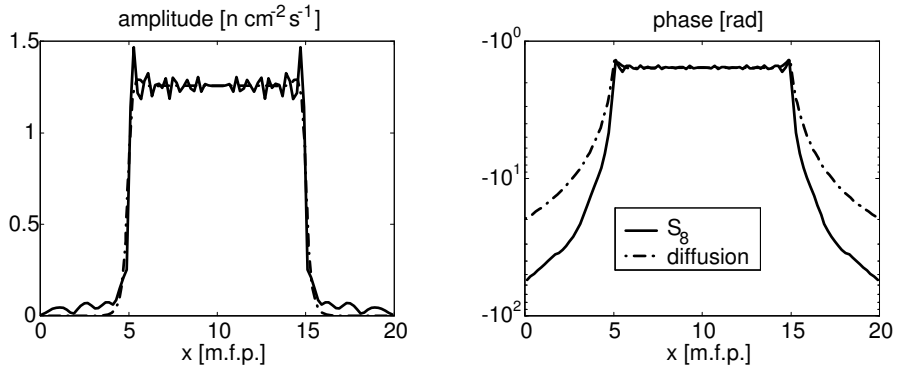

Fig. 9: Comparison between transport and diffusion solutions ($c = 0.9, \omega/v = 10$ mfp^{-1}).

The following results concern calculations run for a configuration typical of the Masurca system for the MUSE experiment. Cross section data have been supplied by ENEA through ERANOS calculations [7]. Fig. 10 and 11 report transport and diffusion results, respectively, for a one-group calculation. Diffusion seems to be inadequate to represent the behavior of the amplitude of the response. Figures 12 and 13 plot the results for a MUSE three-group calculation. Also in this case diffusion is inadequate. As expected, the transport distribution for the amplitude is by far more peaked around the source zone.

4. CONCLUSION

A study of the role of transport effects in the interpretation of source oscillated experiments in subcritical systems is performed by determining the persistent shape of the neutron distribution as solution of the transport problem in the frequency domain, i.e. with an apparent (complex) total cross section as $(\Sigma + i\omega/v)$. The analysis allows the identification of situations in which diffusion theory is inadequate and transport effects need to be accounted for, with special reference to the MUSE experimental configuration.

ACKNOWLEDGMENTS

This work is being performed in a collaboration activity with ENEA-Casaccia, Roma, Italy, within the MUSE project, supported by the European Union through the Fifth Framework Program.

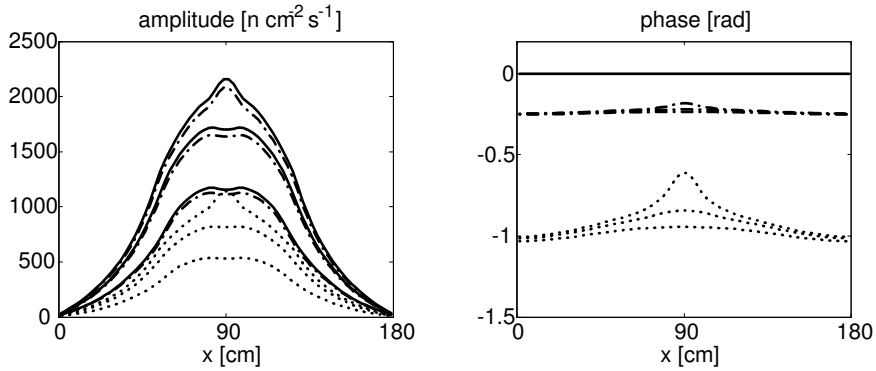

Fig.10: One-group solution for the MUSE configuration in transport model. Amplitude and phase of the response along the x axis are represented for different values of the y coordinate (from top to bottom: on the symmetry line, at 3/8 and at 1/4 of the edge from the symmetry line) and for different frequencies (solid lines: $f = 0\ Hz$; dashed-dotted lines: $f = 1\ kHz$; dotted lines: $f = 10\ kHz$).

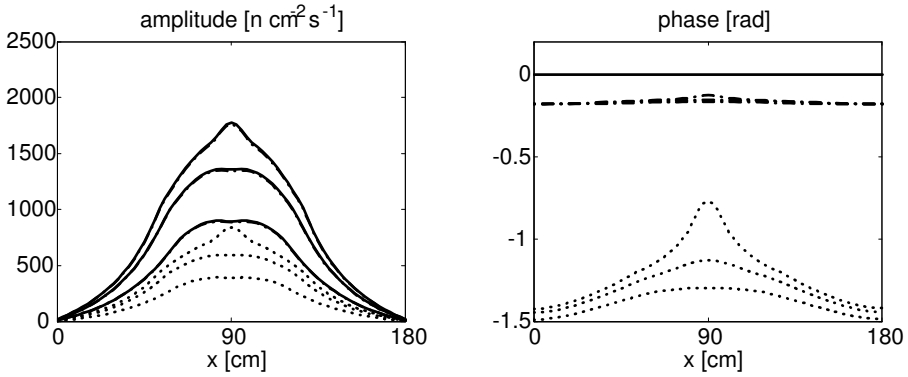

Fig.11: Monokinetic solution for the MUSE configuration in diffusion approximation. Curves are identified as in Fig. 10.

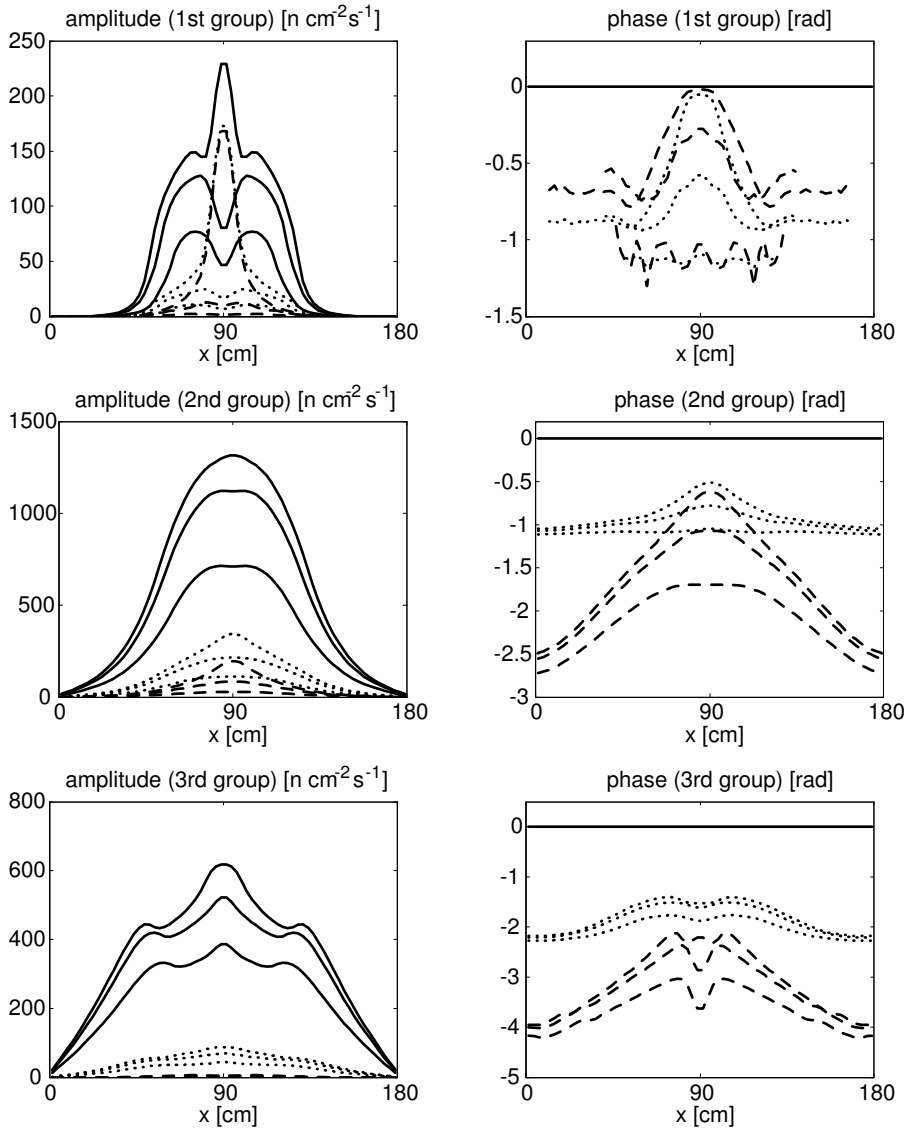

Fig.12: Three-group solution for the MUSE configuration in transport.

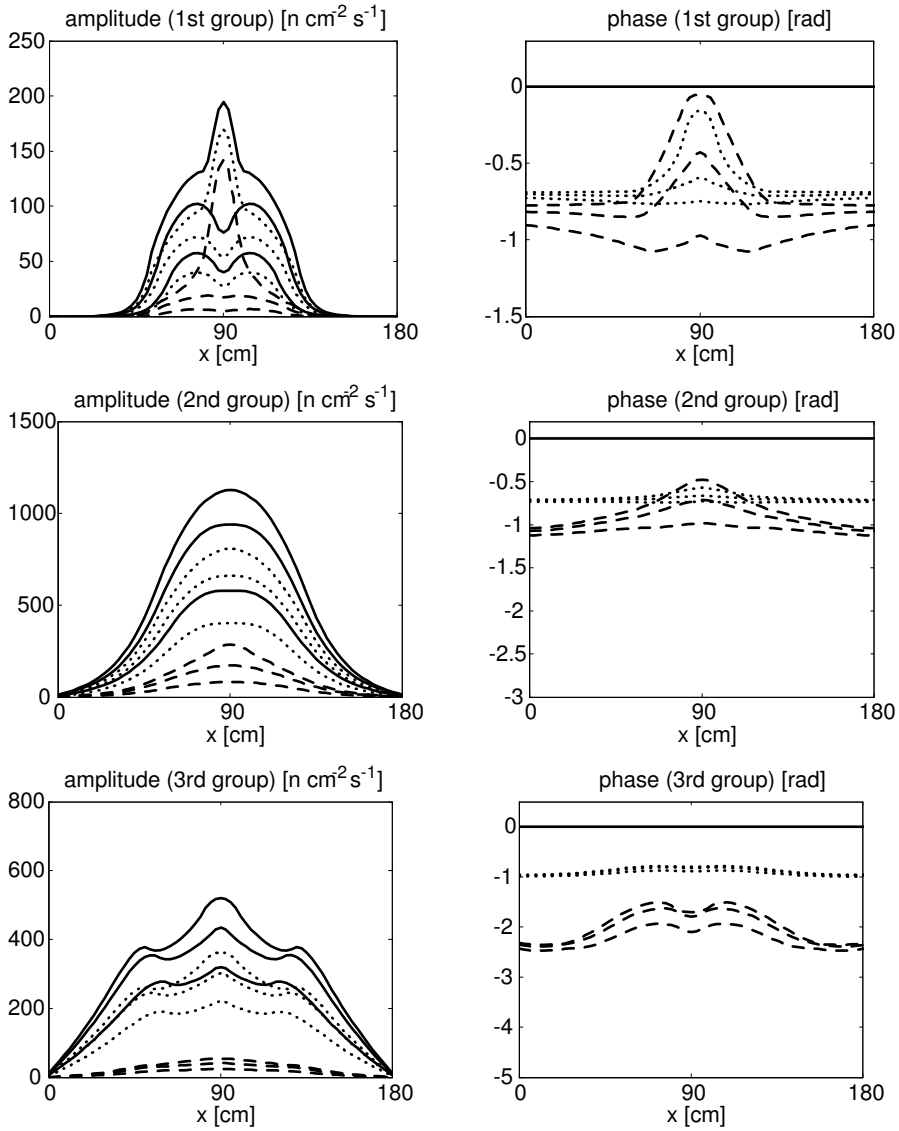

Fig.13: Multigroup solution for the MUSE configuration in diffusion approximation. Curve identification as in Fig. 10.

REFERENCES

1. R.G. Soule, Experimental validation of the neutronic characteristics of the subcritical multiplying medium of an ADS: the Muse experiment, *Proceedings of the Topical Meeting on Accelerator Applications/Accelerator Driven Transmutation Technology and Applications (AccApp/ADTTA 01)*, Reno, November 12-15 (2001).

2. M. Carta et al., Monitoring of subcriticality level in accelerator driven systems: harmonic modulated source - spatial source jerk intercomparison, *Proceedings of the In-*

ternational Conference on Mathematics and Computation, Reactor Physics and Environmental Analysis in Nuclear Applications, Madrid, September 27-30,**1**, pp. 596-605 (1999).

3. E.E. Lewis, W.F. Miller, *Computational methods of neutron transport*, Wiley, New York (1984).
4. E. Larsen, *Acceleration of high-order S_N equations using low-order S_N operators*, LA-10189-PR, Los Alamos National Laboratory (1983).
5. J.E. Morel, T.A. Manteuffel, An angular multigrid acceleration technique for S_N equations with highly forward-peaked scattering, *Nuclear Science and Engineering*, **107**, 330-342 (1991).
6. S. Dulla, *Studio neutronico di sistemi sottocritici in teoria del trasporto*, Master Thesis (in Italian), Politecnico di Torino (2001).
7. M. Carta, Personal communication (2002).